MOSAIC: A Multiwavelength Optical Subcarrier Multiplexed Controlled Network

Roberto Gaudino, May Len, Geoffrey Desa, Michael Shell, *Member, IEEE*, and Daniel J. Blumenthal, *Senior Member, IEEE*

***Abstract*— The experimental demonstration of MOSAIC, a reconfigurable WDM add/drop network with subcarrier multiplexed control, is presented. The MOSAIC network implements the optical layer protocol to support bit-rate transparent multichannel lightpaths. Two types of add/drop multiplexers are implemented and combined in a three-node experiment. Multihop lightpaths are established giving an end-to-end bit error rate of better than 10^{-9} at 1.2 Gbps. The reconfigurable add/drop multiplexer is based on a novel dilated 2×2 acoustooptic filter switch crossconnect and an analog optoelectronic crossconnect that drives a ten-wavelength laser array transmitter up to 2.5 Gbps per wavelength. The fixed wavelength add/drop multiplexer utilizes a fast digitally tunable laser transmitter. Both add/drop multiplexers support bit-rate transparent 2R optoelectronic regeneration as well as wavelength translation. Subcarrier multiplexing on each wavelength is used to support channel state monitoring and channel equalization as well as transmission of digital network control information. Systems experiments demonstrate cascaded 2R optoelectronic regeneration with wavelength translation and cascaded multichannel optical switching with up to seven hops. It is shown that combining cascaded 2R optoelectronic regeneration with cascaded multichannnel optical switching can be used to balance jitter accumulation and amplified spontaneous emission generated amplitude noise to yield high signal-to-noise ratio for lightpaths.**

***Index Terms*—Optical add/drop multiplexers, optical networks, optical subcarrier multiplexing, optical transport networks, reconfigurable add/drop multiplexers, transparent optical networks, wavelength division multiplexing.**

I. Introduction

RECONFIGURABLE wavelength division multiplexed (WDM) add/drop fiber transport networks have the potential to satisfy the demands of future broadband communications applications [1]. Reconfigurability in the add/drop multiplexers will result in increased network configuration flexibility, remote provisioning, and protection switching capabilities.

Manuscript received July 12, 1997; revised April 1998. The work of R. Gaudino was supported by a Grant from AEI (Associazione Elettrotecnica Italiana). The work of D. J. Blumenthal was supported by a National Young Investigator Award (ECS-94-57148), a DARPA DURIP award (DAAH04-96-1-0346), and a Grant from the State of Georgia Research Alliance.

R. Gaudino is with the Dipartimento di Elettronica, Politecnico di Torino, Coso Duca degli Abruzzi 24, 10129, Torino, Italy.

M. Len, G. Desa, and M. Shell are with the Georgia Institute of Technology, Atlanta, GA 30332-0250 USA.

D. J. Blumenthal is with the Optical Communications and Photonic Networks Laboratory, Department of Electrical and Computer Engineering, University of California, Santa Barbara, CA 93106 USA (e-mail: danb@ece.ucsb.edu).

Publisher Item Identifier S 0733-8716(98)05733-3.

Second-generation WDM optical transport networks must set up and maintain lightpaths that support the optical network layer in the network hierarchy [2], [3]. At the physical layer, these lightpaths may incorporate optical and electronic switching, signal regeneration, channel equalization, and wavelength conversion to ensure network scalability and add/drop node cascadability. Over the last several years, multiple WDM transport network testbed demonstrations have been reported [4]–[7].

In this paper we describe the design, implementation, and demonstration of the MOSAIC-network reconfigurable add/drop WDM testbed. This testbed was designed to study the issues of scalability, cascadability, bit-rate transparency, the tradeoffs between optical and electronic switching, and optoelectronic wavelength translation. The MOSAIC testbed was also designed to investigate network element functionality and the support systems needed to integrate enabling technologies into a network environment. In Section II we describe the relationship between MOSAIC and the optical layer protocol stack. In the same section we also describe the add/drop multiplexer (ADM) node design. In Section III, we describe the ADM node subsystems in further detail and report several experimental results including input channel monitoring, multichannel bit error rate (BER) measurement of a dilated acoustooptic tunable filter (AOTF) switch, optical channel equalization, and bit-rate transparent operation of a optoelectronic-optical crossconnect. Section IV describes results of network level demonstrations including cascaded, bit-rate independent, multihop optical bypass and cascaded, bit-rate independent, optoelectronic-optic (OEO) bypass with wavelength translation. Finally, we demonstrate lightpath establishment in a three-node ring network that traverses 150 km fiber and multiple ADM's with optical and optoelectronic drop-and-continue operations, optical bypasses and optoelectronic-optic wavelength translation with 2R regeneration.

II. MOSAIC Architecture

MOSAIC supports the optical layer of second generation optical networks [2], [8]. The optical layer provides *lightpaths*, or end-to-end connections, across the network [3], [9], [10] with dedicated use of an entire wavelength per link in a path between source and destination. For each lightpath, the full bandwidth of a wavelength per link is provided to the higher layer.

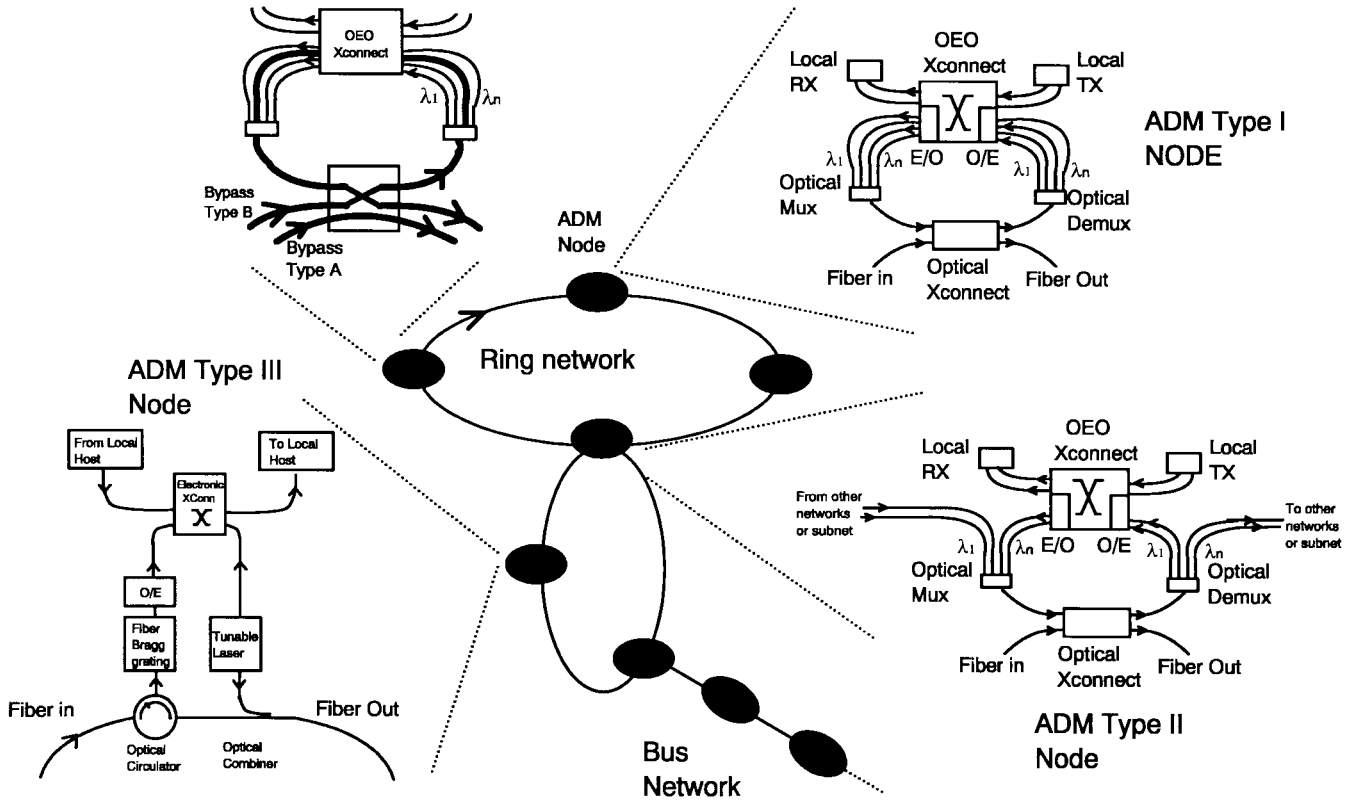

Fig. 1. MOSAIC WDM add/drop transparent network architecture illustrating three types of ADM nodes. Optical and OEO bypass with wavelength translation are also illustrated.

MOSAIC is an add/drop multiwavelength network that may be connected in a ring or bus fashion as shown in Fig. 1. Three types of ADM's have been designed and implemented and are shown in Fig. 1. Type I and II ADM's support multiwavelength add/drop, level regeneration, and wavelength-translation. The Type I ADM can pass a lightpath from the input fiber to the output fiber or add/drop data between the network and a local host. The Type II ADM, in addition to performing the basic functions of a Type I ADM, can route a lightpath to another optical network or subnet. The Type III ADM drops a single fixed wavelength and can add or wavelength translate to one of any network supported wavelengths.

The Type I ADM incorporates an OEO crossconnect based on arrayed detectors and a multiwavelength source fully connected to the mux/demux and the local host. The Type II ADM maintains a subset of the mux/demux channels in optical format for routing to other networks. The Type III ADM utilizes a fixed wavelength drop port and wavelength tunable transmitter. Two bypass modes, A and B, are supported and are shown in Fig. 1. Bypass mode A is used to optically route a wavelength without wavelength translation. Bypass mode B mode, also referred to as *drop-and-continue*, is used to route a wavelength through the bit-rate transparent OEOXC with level restoration and the option to perform wavelength translation. The Type B bypass mode also supports digital broadcasting [7].

The MOSAIC network elements (e.g., ADM's) contain hardware components that are applicable to a broader class of optical networking architecture and specific hardware components that are designed for MOSAIC. The four basic components within a MOSAIC ADM are a WDM optical crossconnect (WDM-OXC), an optoelectronic-optical crossconnect (OEOXC), a wavelength mux/demux, and a node control processor (NCP). The WDM-OXC performs the following general functions: rearrangable optically transparent crossconnections on a per wavelength basis, monitoring which wavelengths are present at the ADM input, extraction of control data on the incoming wavelengths, and equalization of the per wavelength power at the ADM output. Hardware that is specific to MOSAIC involves detection and decoding of subcarrier signals using multichannel RF/digital receivers at the ADM input and multichannel RF receivers for channel equalization at the ADM output. The OEOXC performs the general functions of a rearrangable analog electronic crossconnect with optoelectronic conversion and thresholding. The OEOXC outputs are wavelength division multiplexed, and therefore, wavelength conversion can be performed. Functions in the OEOXC specific to MOSAIC involve reinsertion of subcarrier multiplexed control signals with the retransmitted data channels. The wavelength mux/demux and NCP are generic functions applicable to most optical network architectures.

A. Subcarrier Signaling and Channel Monitoring

Several techniques to communicate control information in a WDM optical network have been studied and implemented including in-band signaling [4], out-of-band signaling on a separate control wavelength [11] and optical subcarrier multiplexing (OSCM) [12], [13].

Out-of-band signaling by OSCM is used in MOSAIC to achieve multiple functions simultaneously including wavelength identification, wavelength power monitoring and digital control signaling. In comparison with transmitting control on a separate wavelength, the subcarrier per wavelength approach supports distributed network control with a synchronous recovery of wavelength identification, wavelength power, and control data using a common circuit and requires only a single laser at each users transmitter and a single photodetector at each monitoring or detection point. The subcarrier portions of the transmitters and receivers can be fabricated using low cost monolithic-microwave integrated circuit (MMIC) technology that has been developed for wireless communications [13].

Potential limitations to OSCM include fiber nonlinearities and dispersion and detector saturation. Crosstalk due to fiber four-wave mixing [14] is low as there is a single subcarrier per wavelength and the relative power of the subcarrier component is much less than the baseband component of the optical signal. Signal cancellation and fading due to dispersion can be overcome using single sideband subcarrier modulation techniques as demonstrated in [15]. Monitoring of many subcarrier channels using a single photodetector can be achieved with new high power traveling wave photodetector designs [16].

B. ADM Node Architecture

The main ADM components are shown in Fig. 2(a) and (b) and are outlined below.

1) The WDM Optical Crossconnect (WDM-OXC): Used in both Type A and B bypass states, the WDM-OXC consists of four subsystems: an in-line optical amplifier, a WDM input channel state monitor, a WDM optical switch, and a WDM channel equalizer. All wavelengths at the node input are amplified using an erbium doped fiber amplifier (EDFA). The WDM input channel state monitor is used to determine the set of wavelengths present at the ADM input and to decode channel control information. Individual wavelengths are tagged with a subcarrier frequency that corresponds to that particular wavelength. A portion of the optical input is tapped at the WDM-OXC input, photodetected, and demodulated using a parallel channel subcarrier receiver to recover network and channel control information. Type I and II ADM's use the WDM dilated 2×2 acoustooptic switch architecture reported in [17] and [18]. Type III ADM uses a broadband optical circulator and wavelength selective filter to drop a single wavelength and bypass the remaining wavelengths. The channel equalizer measures the power per wavelength at the ADM output and adjusts AOTF RF drive power per channel.

2) The OEO Crossconnect (OEOXC): The OEO crossconnect (OEOXC) is used to implement a Type B bypass with the capability of bit-rate independent optoelectronic wavelength translation with 2R signal regeneration or add/drop with the local host. The Type I and II OEOXC's contain an analog electronic crossbar switch with output thresholding (2R), a photodetector array, and a WDM laser array configured similar to [7]. The OEOXC in the Type III ADM uses a wide wavelength tunable laser transmitter [19] and single photodetector in place of the multiwavelength laser array and arrayed receiver. The 2R electronic crossbar switch is an $(N+M)\times(N+M)$ strictly nonblocking bit-rate transparent switch with N input and N output ports interfacing to a $1 \times N$ photodetector array and a $1 \times N$ multiwavelength laser array, respectively. The remaining M input and M output ports are used to interface to the local host. For the Type I and II ADM's, $N = W$, the number of network wavelengths; for the Type I ADM, $N = M = 1$. The electronic crossbar switch used in our experimental demonstration is a 2R reconfigurable regenerator that is digitally transparent up to 2.5 Gbps.

3) The WDM Multiplexer and Demultiplexer: The WDM multiplexer and demultiplexer is responsible for separating and combining lightpaths in add/drop or bypass paths. In the Type I ADM node, the number of inputs/outputs to the mux/demuxes are equal to the number optical inputs to the OEOXC. For a Type II ADM, the mux/demux size is greater than the OEOXC optical inputs so that a subset of lightpaths may be remultiplexed and forwarded to another network or subnet as shown in Fig. 1. The Type III ADM utilizes a filter that routes one wavelength into the node and passes or reflects the remaining wavelengths to the ADM output.

4) The ADM Node Control Processor (NCP): The NCP coordinates all functions within an ADM node and processes network management and control information. The NCP coordinates signal connection requests, keeps track of the ADM input state, acknowledges availability of local lightpath resources, and controls the state of the WDM-OXC and OEOXC. Network signaling is carried out using optical subcarrier multiplexing where an RF subcarrier is modulated onto each wavelength in addition to the baseband information. Each wavelength contains a unique subcarrier used for wavelength identification [20] and carries low bit rate (order 100 Mbps) data for network and channel control information.

C. Optical Layer Implementation

The MOSAIC ADM node structure can be mapped onto the International Telecommunication Union (ITU) recommended optical layer for second-generation optical networks [2], [3], [8]. In this model, the optical layer provides lightpaths to higher protocol layers (e.g., SONET/SDH, ATM). We have established the relationship between the three optical layers and MOSAIC node functions as shown in Table I.

The optical channel (OC), or lightpath layer, is responsible for end-to-end routing of lightpaths. The OC layer determines the best paths for a given lightpath including combinations of bypass modes and controls the optical multiplex section described below. The optical multiplex section (OMS) layer is responsible for configuring the node in an add/drop or bypass state for each lightpath. This layer is also responsible for separating and combining wavelengths and performing the wavelength translation function. The optical amplifier section (OAS) layer handles the link level functions of data transmission and ensures the necessary SNR is delivered between lightpath end points. This layer can also decide on optimal combinations of optical and OEO bypass to maximize the lightpath SNR.

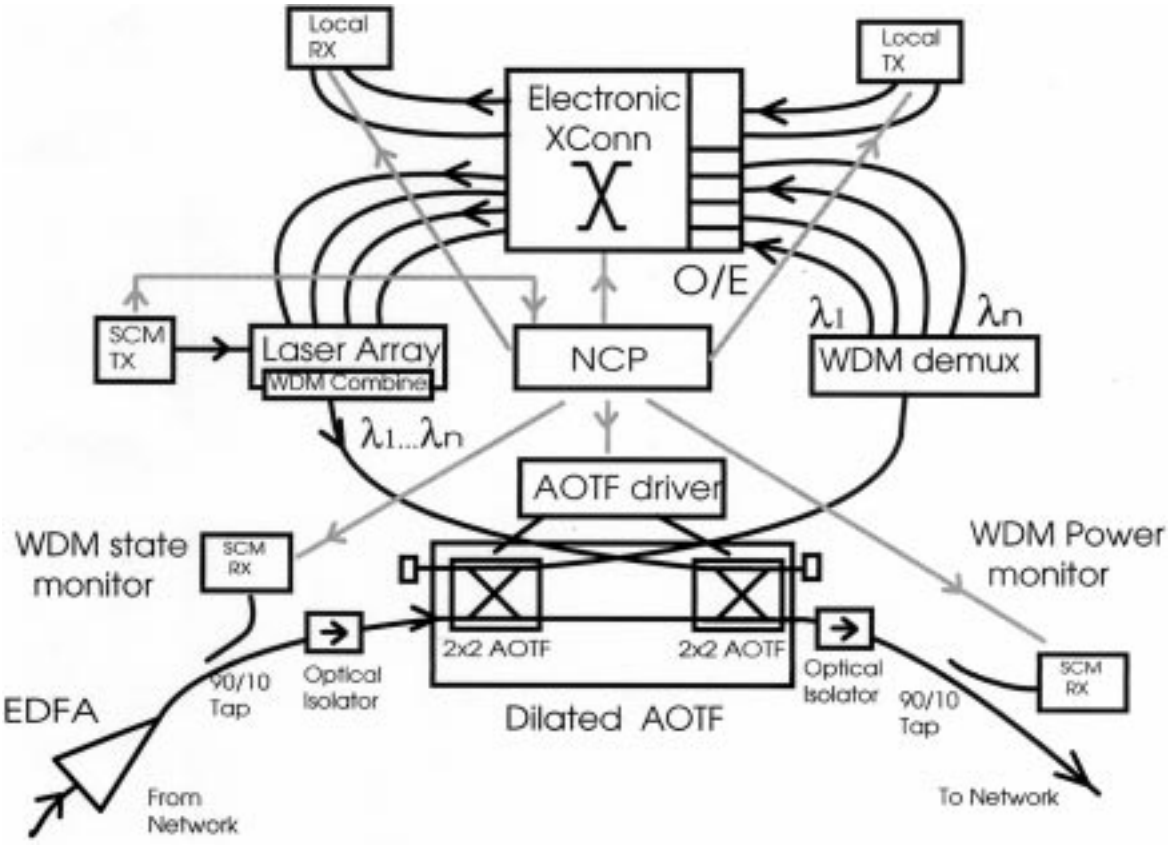

(a)

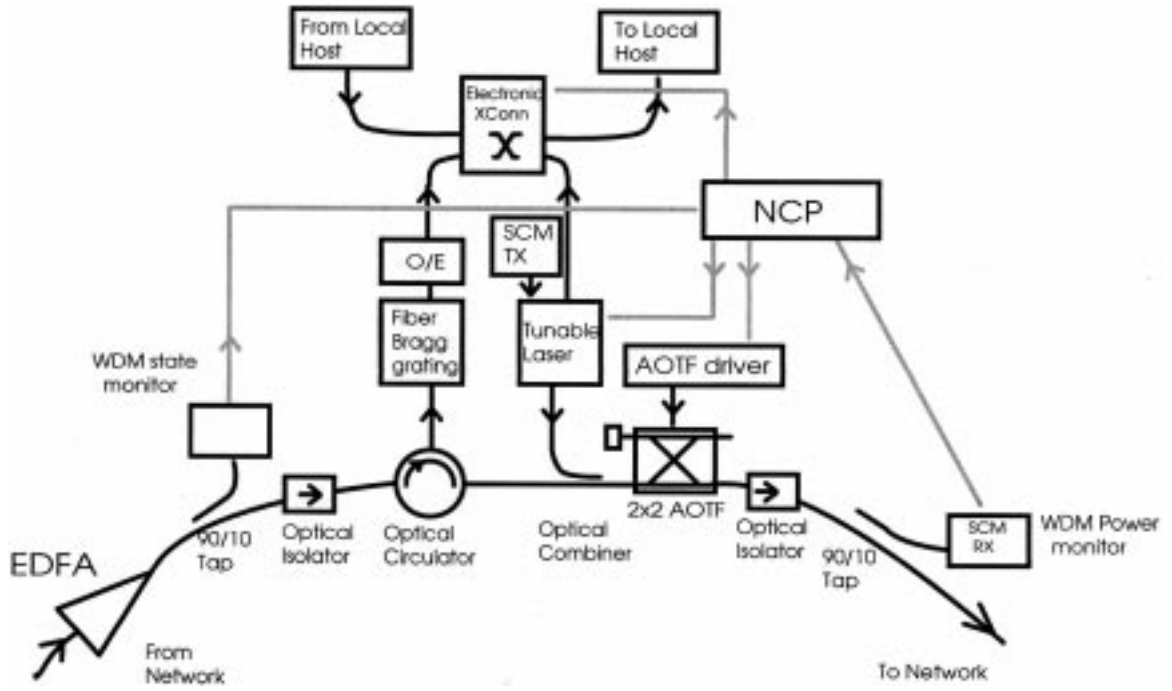

(b)

Fig. 2. ADM node subsystems and components: (a) Type I: multichannel add/drop with wavelength translation and optical and 2R OEO switching and (b) Type III: single channel drop with single tunable wavelength add and 2R OEO wavelength translation.

An example of how the MOSAIC optical layer supports two simultaneous lightpaths is shown in Fig. 3. Lightpaths A and B, indicated in the figure, are add/dropped at different nodes and traverse a different combination of network elements (NE's). For each lightpath, the OM section is configured as a Type A or Type B bypass. In each case, the originating and

TABLE I
OPTICAL LAYERS

Layer	Functions	Physical components
Optical Channel OC	• End to end routing of lightpaths • Signaling connection requests • Monitoring connection requests • Monitoring network state • Acknowledge of lighpath availability • Control of resources to set lightpath • Establish routing map	• Network controller • Baseband transmitter and receivers • Subcarriers transmitter and receivers • Input channel state monitor
Optical Multiplex Section OMS	• Configure mux section as bypass Type A or B, add or drop • Wavelength conversion • Wavelength separation	• Dilated AOTF • Electronic cross-connect • Optical Mu/Demultiplexers
Optical Amplifier Section OAS	• Optical amplification • Channel equalization • SNR quality monitoring • Transmitter • Receiver • Regeneration (level and/or timing restoration, OEO and all-optical)	• EDFA • Dilated AOTF • Baseband transmitter and receivers • Subcarrier transmitter and receivers • Electronic cross-connect

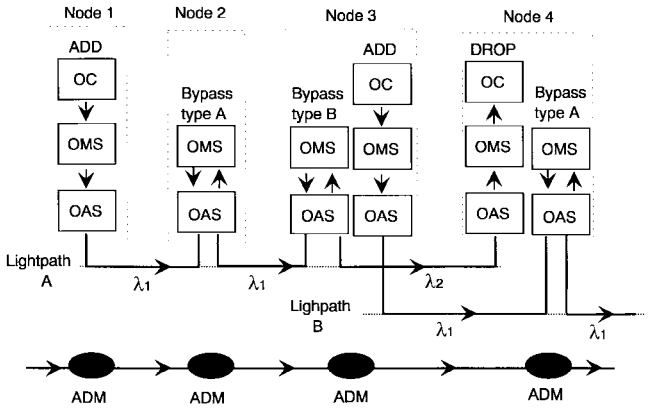

Fig. 3. Example of MOSAIC supporting two lightpaths using ITU optical layer model.

terminating NE's pass the lightpath through the OC section and in all cases the lightpath passes through the OM and OA sections. In this example, lightpath A is added to the network on λ_1 at node 1 and lightpath B is added to the network on λ_1 at node 3. Lightpath A traverses one node in the Bypass A state and one node in the Bypass B state that is used to convert the wavelength to λ_2. This wavelength translation is needed prevent blocking of lightpath A. Node 3 is configured as a bypass Type B node for lightpath A and an add node for lightpath B. Lightpath A is dropped at node 4, and lightpath B is Type A bypassed at node for further routing in the network.

III. MOSAIC SUBSYSTEMS

In this section we describe in more detail the WDM-OXC and OEOXC subsystems and present experimental results. The optical multiplexer is internal to the laser array chip, while a Lucent 1×8 silica on silicon integrated optic router was used as the wavelength demultiplexer and is shown in Fig. 5.

A. WDM Optical Crossconnect (WDM-OXC)

Type I and II OXC's allow reconfigurable WDM add, drop, and bypass functions. The Type III OXC provides similar functions using fixed wavelength drop, and single tunable wavelength add and translation. Subsystem implementations and demonstrations are described below:

1) Optical WDM Channel Monitoring: With OSCM, only a single photodetector is required to monitor the state and control information of all incoming channels. A fiber tap is used to direct a fraction of the input optical power to the photodetector as shown in Fig. 4. The recovered electrical signals are demultiplexed using heterodyne frequency down conversion and amplitude detection as shown in Fig. 4. The four-channel subcarrier receiver is shown in the experimental ADM node in Fig. 5. Local VCO's provide continuous tuning from 4.8 to 6.2 GHz. MMIC mixers are used to down-convert RF channels to 300 MHz. Bit recovery of 100 Mbps control and detection of average subcarrier power is achieved using LPF's.

2) Multichannel Dilated WDM Optical Switch for Type I and II ADM's: The multichannel WDM-OXC is based on a novel dilated switch constructed from two cascaded 2×2 AOTF switches [18] and is shown in Fig. 6. AOTF technology has evolved significantly over the last several years [21]. Primary limitations in dense WDM systems are related to bit errors induced during multichannel exchange/bypass operations [22], [23] and may be overcome using techniques like spatial and/or wavelength dilation [24]. The MOSAIC dilated optical switch consists of cascaded, polarization independent, fully integrated apodized AOTF's made by Pirelli Cavi S.p.A [17] with filter bandwidth and sidelobe suppression designed for a 3.2 nm spaced WDM network. The first stage independently routes wavelengths $[\lambda_i, \cdots, \lambda_j]$ to the second stage or to the wavelength demultiplexer. The second stage is used to improve the signal extinction ratio, decrease inter- and intrachannel crosstalk from the first stage, and to route $[\lambda_n, \cdots, \lambda_m]$ from the OEOXC to the network. The switching state of the dilated AOTF switch is determined by the applied RF frequencies $[f_i, \cdots, f_j]$ to both AOTF switches. This configuration exhibited better than 30 dB rejection on the dropped channel and a suppression of more than 18 dB on the sidelobes at the drop port. This rejection is further improved by the WDM

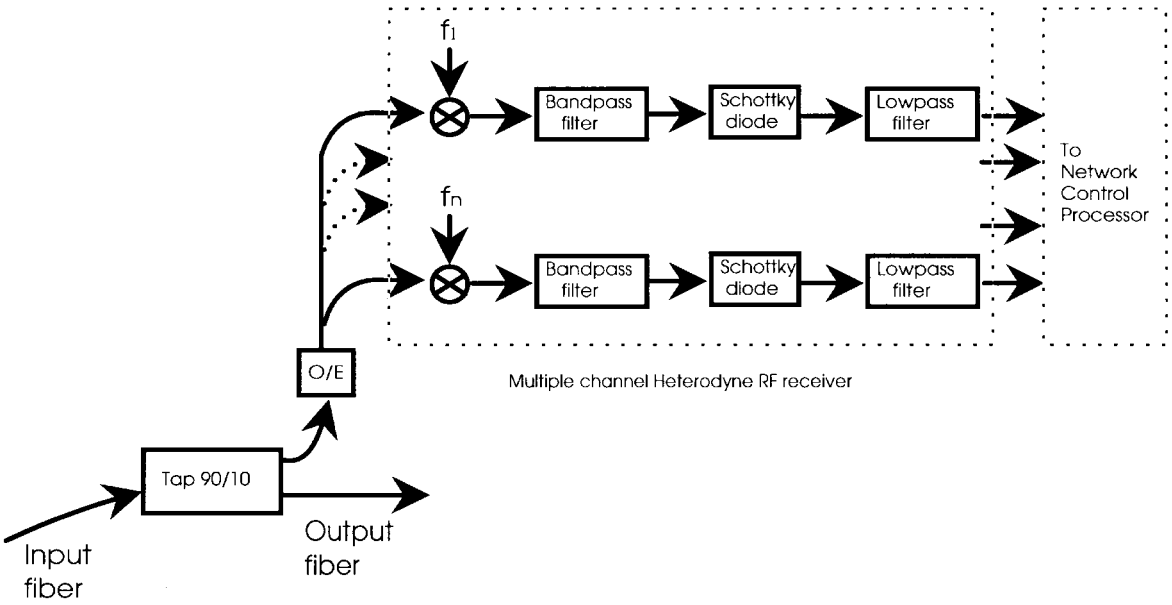

Fig. 4. Schematic for subcarrier-based WDM channel monitoring and channel equalization subsystems.

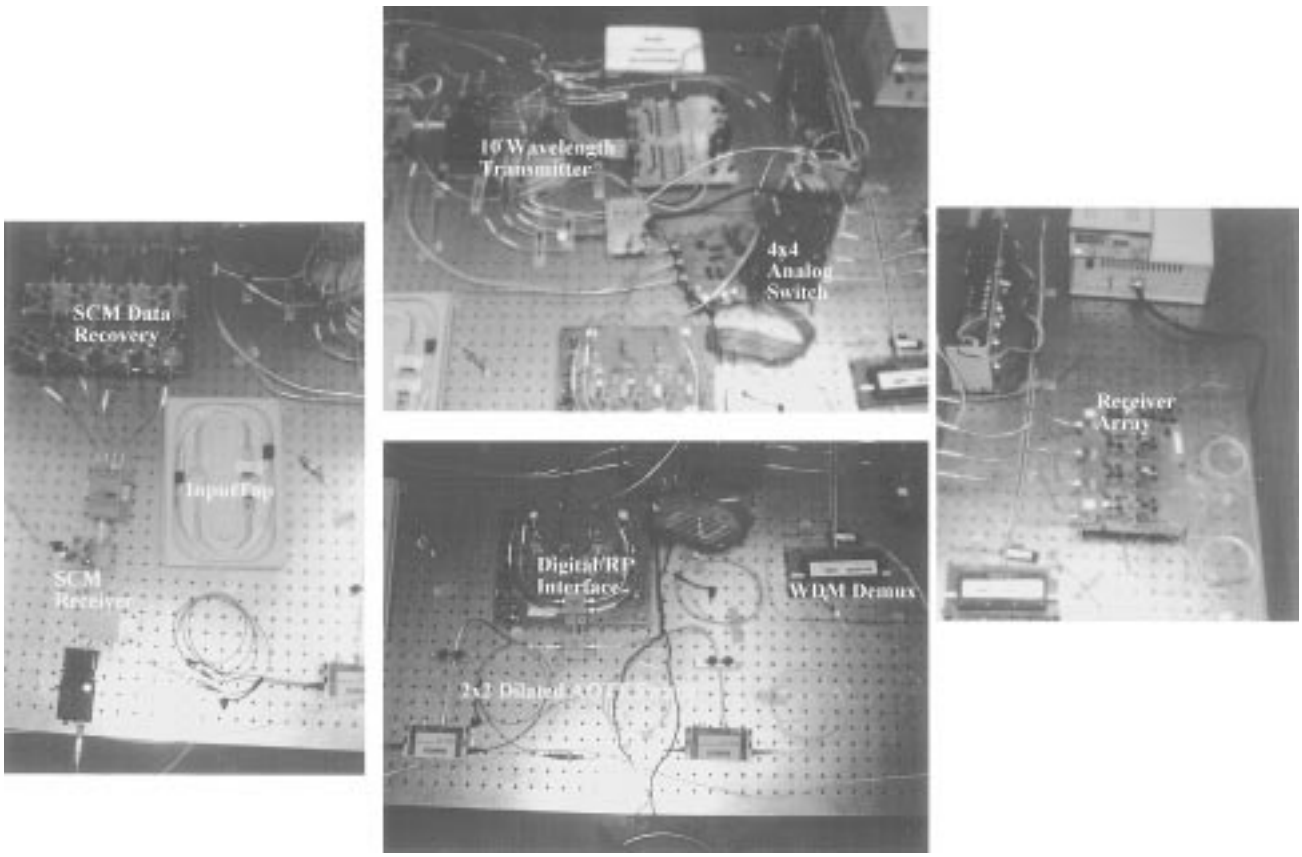

Fig. 5. Photograph of experimentally demonstrated Type II ADM.

demux with a measured power penalty less than 0.3 dB at $P(e) = 10^{-9}$ for coherent and incoherent crosstalk.

Demonstration of multichannel add/drop is shown in Fig. 7. Four WDM channels were applied at the input [Fig. 7(a)] and channels 1 and 3 were dropped. The optical signals at the second stage output are shown in Fig. 7(b) with the dropped channels rejected by more than 30 dB. The dropped channels after the demux are shown in Fig. 7(c) and (d) demonstrating better than 30 dB isolation.

The performance of an AOTF switch that is controlled with multiple RF frequencies [22], [23] is a key issue for multichannel ADM's. Fig. 8(a) shows the measured BER as a function of power at the drop port when a signal at $\lambda_0 = 1556.8$ nm was dropped by applying an RF signal at

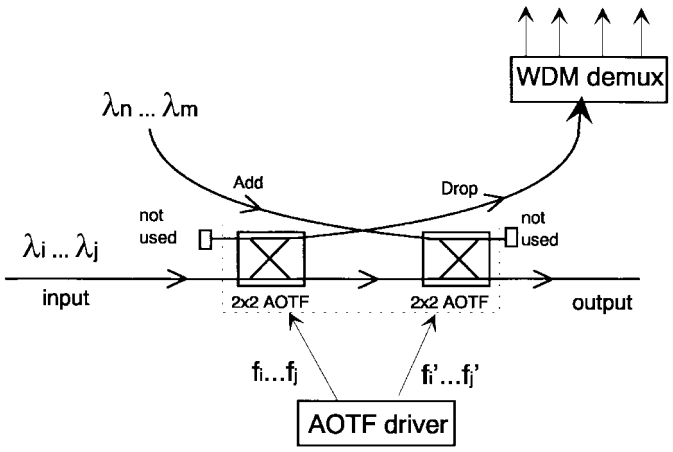

Fig. 6. Schematic of the dilated 2 × 2 AOTF switch and the optical demux.

$f_{\mathrm{RF},0}$ and adding a second RF signal at $f_{\mathrm{RF},1}$. The different curves correspond to different values of $\Delta f = f_{\mathrm{RF},0} - f_{\mathrm{RF},1}$. For $\Delta f = 400$ kHz ($\Delta\lambda = 3.2$ nm) the power penalty at BER $= 10^{-9}$ is greater than 2 dB. The penalty reduces to below 0.3 dB for $\Delta f = 600$ kHz allowing alternate channels in a 3.2 nm system to be dropped simultaneously with acceptable BER, constraining the current implementation to alternate channel dropping.

Another degradation mechanism is coherent, or in-band, crosstalk [25], [26], which occurs when a channel at wavelength λ_i is switched off the network and a new channel is added at a nominally the same wavelength. This signal will be further degraded in the presence of other acoustic frequencies spaced by Δf as shown in Fig. 8(b). The penalty due to optical coherent interference was measured for our node architecture to be less than 0.5 dB when a single RF signal was applied and around 1 dB when a second frequency at $\Delta f = 800$ kHz was applied.

3) Fixed Wavelength Drop for Type III ADM: This add/drop utilizes a fiber recirculator, Fabry–Perot fiber filter (FPFF), and 2 × 1 combiner as shown in Fig. 2(b). The FPFF passes a single WDM channel to the OE converter and reflects the remaining channels through the recirculator output port. A new wavelength channel is added using the fiber combiner.

4) Digital/RF AOTF Interface: The digital/RF interface allows the AOTF switching state and attenuation factor per wavelength to be set by the node control processor and is shown in the ADM photograph in Fig. 5. The circuit is based on a digital to multichannel analog/RF converter design that maps digital inputs to a set of RF frequencies each with controllable RF power.

5) Optical Channel Equalization: WDM channel equalization is needed to compensate for signal propagation through cascaded wavelength dependent elements [27]. AOTF's can be used as multichannel variable attenuators to equalize the power level of each wavelength [28] by adjusting the relative RF channel powers.

We have designed and implemented a channel monitoring technique that measures the relative subcarrier RF power at the node output and adjusts the AOTF RF drive signal powers accordingly. Power monitoring is accomplished using an optical tap at the ADM output in conjunction with a subcarrier detection circuit. The measured subcarrier power levels are used to generate error signals at the NCP. The ratio between optical signal power and RF power in the corresponding subcarrier signal is fixed within a specified tolerance for all transmitters in the network. Four-channel WDM power equalization was experimentally demonstrated. Two wavelengths were dropped and two wavelengths bypassed as shown in Fig. 7. The initial 2 dB power unbalance on the input signals was reduced to less than 0.2 dB on all ports. Next, two WDM channels, each carrying a subcarrier tone, were input to the AOTF switch. The input optical and RF power unbalance was measured to be 2.3 dB as shown in Fig. 9(a) and (b). The ratio between total channel power and subcarrier signal power was set at 10 dB for each wavelength. Equalization of the optical channel powers [Fig. 9(c)] to within 0.2 dB as shown in Fig. 9(d).

B. Optoelectronic Crossbar Switch (OEOXC)

Type I and II OEOXC's consist of a multichannel WDM/SCM transmitter, a multichannel receiver and a $(N + M) \times (N + M)$ digitally transparent 2R electronic crossbar switch. Our current version incorporates four 1.22 Gbps OE converters, a 5 GHz 4 × 4 analog switch, and a ten-wavelength, 2.5 Gbps per channel, WDM/SCM transmitter as shown in Fig. 5. The multichannel transmitter allows direct combining of a digitally modulated SCM channel with the baseband channel. The Type III OEOXC utilizes a single OE converter and externally modulated digitally programmable wavelength tunable transmitter.

1) WDM Array Transmitter with SCM: The multichannel WDM transmitter is based on an integrated WDM laser array and combiner [29] with laser array drivers [30]. We packaged the transmitter using a technique that minimizes electronic crosstalk when all ten lasers are simultaneously modulated [31]. The packaged laser array chip and driver arrays are shown in Fig. 10(a). The optical spectra in Fig. 10(b) shows uniform channel power on all the ten channels of the 1.6 nm spaced wavelengths. Modulation of all ten wavelengths at 2.5 Gbps is shown in Fig. 10(c) with electrical crosstalk measured to be 32.1 dB.

Subcarrier modulation was added to each wavelength by wire ORing an ac coupled signal to the baseband driver output as shown in Fig. 11(a). The frequency response of the SCM optical channel was measured to extend beyond 6 GHz as shown in Fig. 11(b). The RF power spectrum of one wavelength channel modulated with baseband (2.5 Gbps) and ASK modulated subcarrier (100 Mbps data on a 5.5 GHz subcarrier) is shown in Fig. 11(c).

2) Digitally Controlled Wavelength Tunable Laser Transmitter: The single channel tunable wavelength transmitter is shown in Fig. 12 and is reported in further detail in [19]. The laser is a four-section GCSR laser that is tunable over a 65 nm range [32] by controlling the current in each of three tuning sections. A digital interface circuit allows fast course-tuning

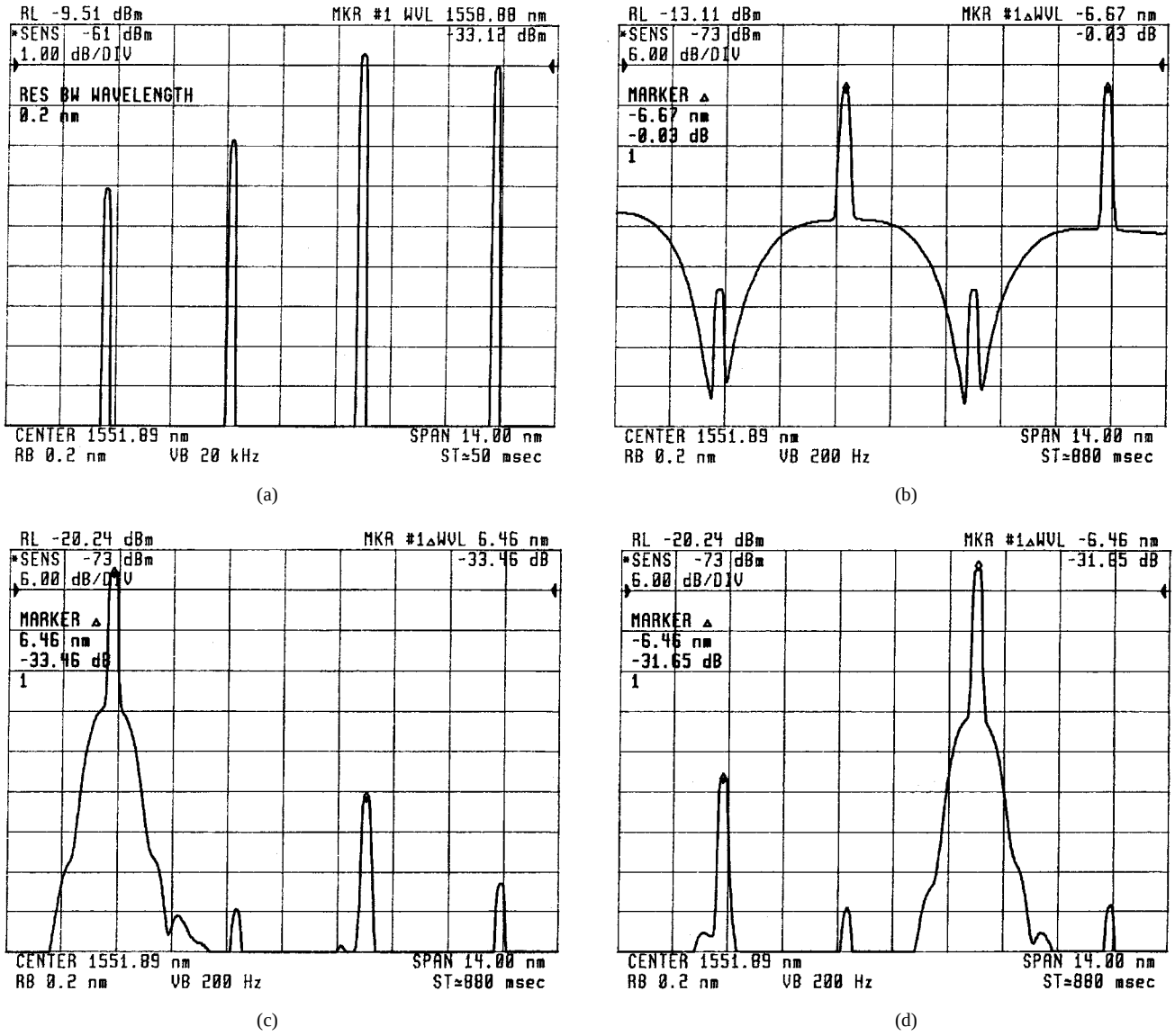

Fig. 7. Demonstration of WDM multichannel add/drop using dilated AOTF 2 × 2 switch: (a) dilated AOTF input, (b) dilated AOTF output, (c) dropped wavelength 1, and (d) dropped wavelength 3.

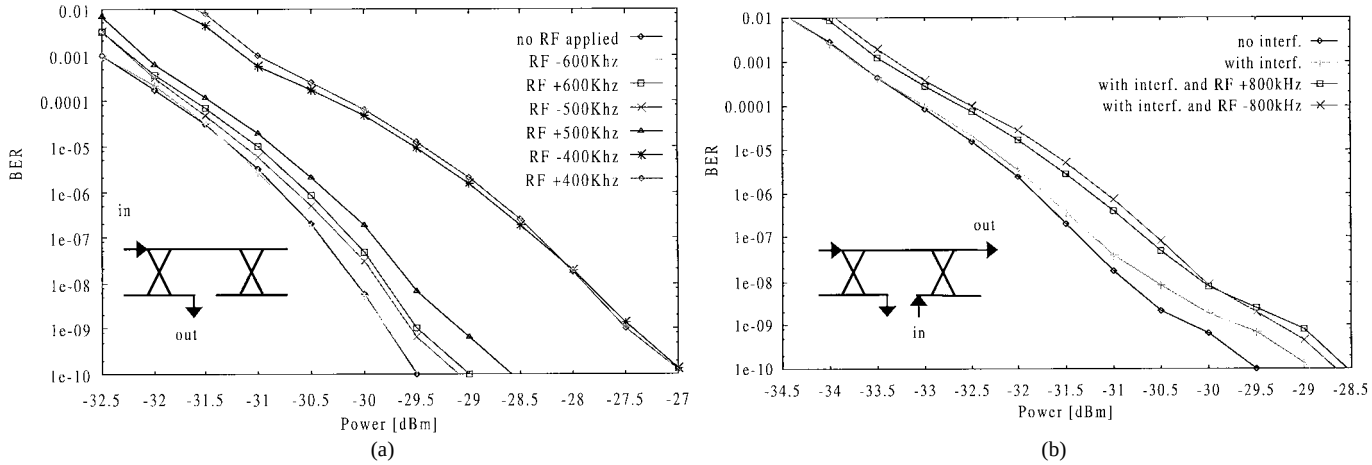

Fig. 8. BER measurement on the dilated AOTF in the presence of multiple RF frequencies: (a) drop port and (b) add port.

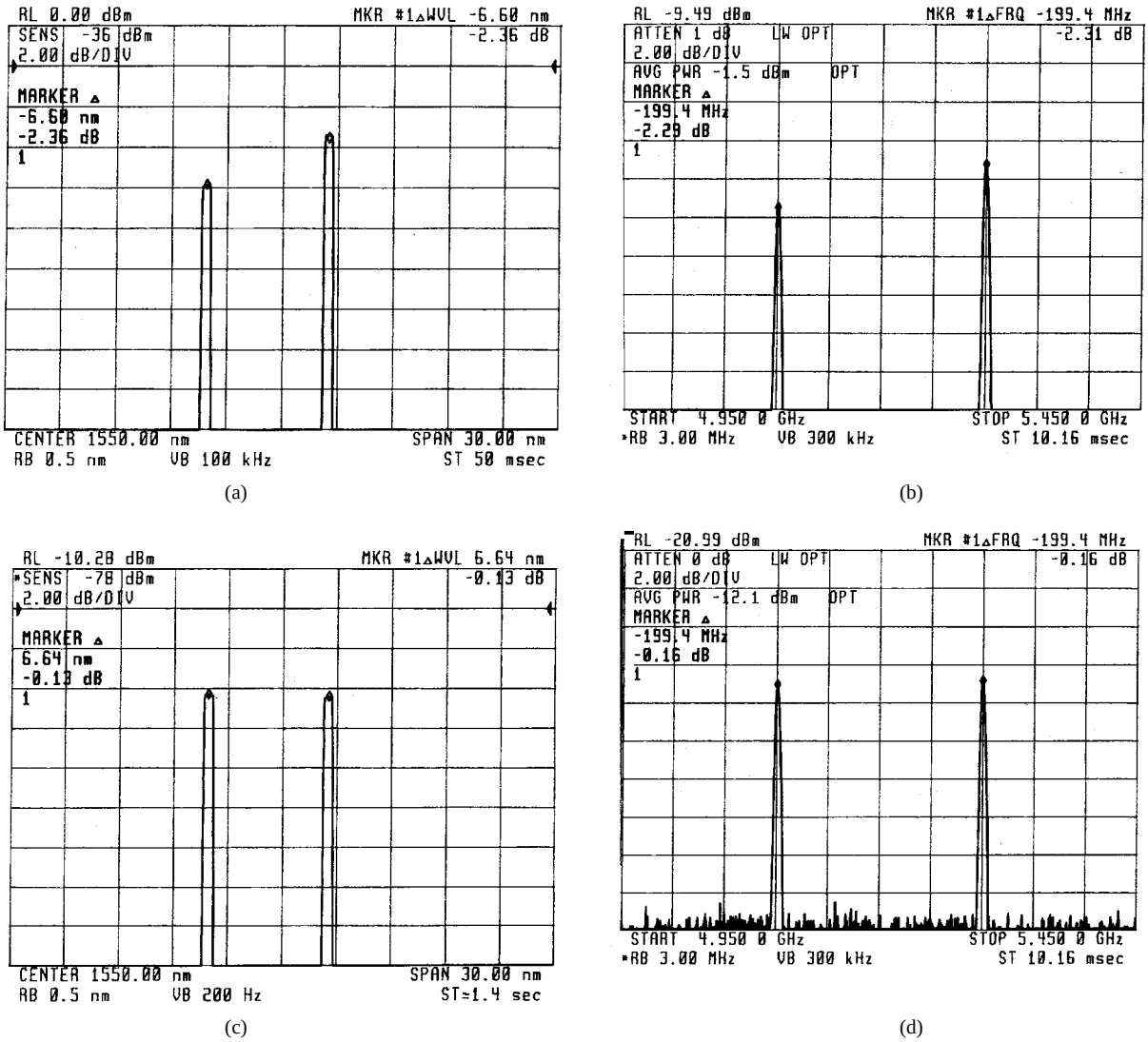

Fig. 9. Two channel equalization using measured subcarrier signal levels: (a) optical input spectrum, (b) electrical input spectrum, (c) optical spectrum after equalization, and (d) electrical spectrum after equalization.

to any network wavelength within approximately 10 ns. The laser output is externally modulated using a lithium niobate integrated optic modulator.

3) 2R Electronic Crossbar Switch: A 4×4 strictly nonblocking electronic crossbar switch has been realized using discrete RF components and is shown in Fig. 5. The resulting input–output transfer function has a 3 dB bandwidth of 3 GHz, an isolation between channel of 40 dB and an insertion loss of 2 dB. The switch outputs are equipped with analog-to-ECL converters for 2R regeneration and compatibility with the laser array drivers.

4) Multichannel Optical Receiver: A four-channel, variable gain, 1.2 Gb/s receiver has been realized and is shown in Fig. 5. It has a sensitivity of -28 dBm at $P(e) = 10^{-9}$. An eight-channel 2.5 Gbps receiver array is currently under development.

5) OEOXC Experimental Demonstration: Transparent switching of 622 Mbps, 1.2 Gbps, and 2.5 Gbps PRBS data streams is shown in the eye diagrams in Fig. 13. The 622 Mbps and 1.2 Gbps switching is OEO while the 2.5 Gbps is electrical only due to the limited bit rate of our receiver array. The results shown are for bar state only but were identical for all possible cross states.

Three experiments were performed to demonstrate the establishment of lightpaths and to study ADM cascadability and scalability issues. The first two experiments were used to investigate the transport level performance of cascaded OEO and optical bypass stages. The third experiment demonstrates a three node MOSAIC ring utilizing a Type II and Type III ADM in conjunction with a simple passive drop port.

A. Cascaded OEO 2R Regeneration with Wavelength Translation

In the first experiment we demonstrated add, drop, and cascaded type B bypass operations. As shown in Fig. 14(a), a baseband signal at 1.2 Gbps is generated on wavelength $\lambda_1 = 1547.5$ nm, optically amplified and added to an optical ring, consisting of 50 km of fiber, an EDFA, and an 8-dB attenuator that was used to simulate the insertion loss of a second ADM node. The received signal is dropped, detected,

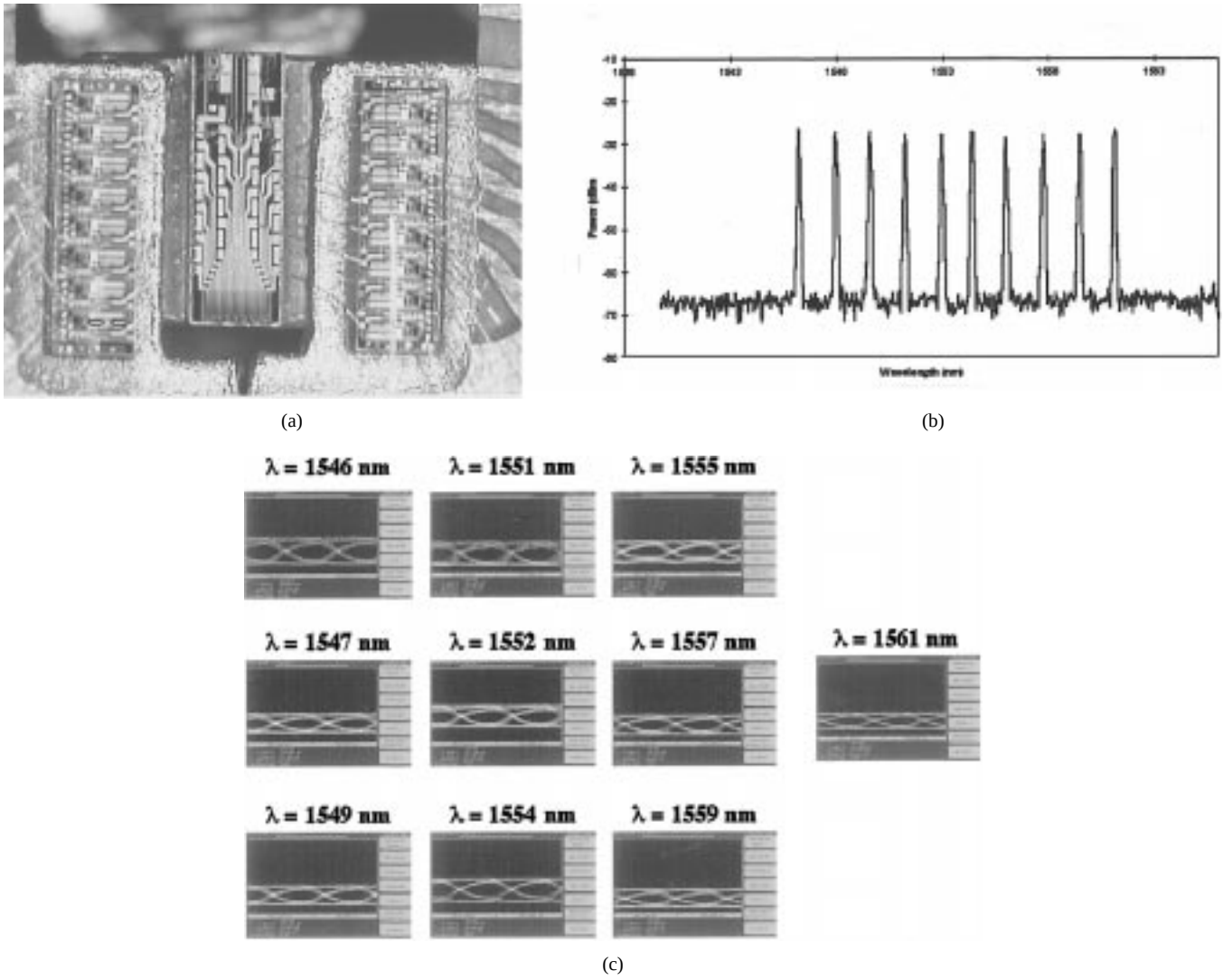

Fig. 10. (a) Packaged multiwavelength laser array transmitter, (b) optical output spectrum of ten wavelengths, and (c) 2.5 Gbps eye diagrams for all ten channels.

2R remodulated, and added to the ring on a second wavelength $\lambda_2 = 1554.0$ nm. After one circulation on the ring, the signal on λ_2 is dropped and detected.

We measured the end-to-end BER, obtaining error free operation for more than 1 h, without requiring setting readjustments. After 1.2 h, the BER degraded to 10^{-7}, due to thermal drift in the laser array and the optical portion of the ADM. Fig. 14(b) shows the eye diagram for λ_1 after the first circulation and the eye diagram for λ_2 after the second circulation is shown in Fig. 14(c). These eye diagrams illustrate the jitter accumulation during cascaded OEO 2R regenerations, resulting in a closure of the eye from the sides and eventually degrading the BER performance [33], [34]. Therefore, the number of 2R OEO regenerations for a lightpath may be combined with optical bypass functions to extend the number of hops.

B. Cascaded Multichannel Optical Bypass

The second experiment, shown in Fig. 15(a), uses a recirculating loop technique to demonstrate cascaded performance of a MOSAICnet ADM in a Bypass Type A configuration. We study the effect of seven passes through the bar state of a dilated AOTF ADM while the two adjacent channels are dropped using RF signals $f_{\mathrm{RF},1}$ and $f_{\mathrm{RF},2}$ spaced by $\Delta_f = f_{\mathrm{RF},1} - f_{\mathrm{RF},2}$ corresponding to a 3.2 nm spacing.

The recirculating loop consisted of a 2×2 coupler, a 75-km-long dispersion shifted fiber, three EDFA's, the dilated WDM AOTF switch, and a broadband optical switch (required to synchronize the loop and gate ASE buildup). The results, in term of Q-value as a function of the number of recirculations, are shown in Fig. 15(b). After seven recirculations we were able to obtain $Q > 6$ [corresponding to $P(e) = 10^{-9}$] with a small penalty observable on the eye diagram when the RF signals are applied. For more than seven recirculations, the loop performance was limited by amplified spontaneous emission (ASE) accumulation. ASE accumulation closes the eye from the upper and lower levels, limiting the number of all-optical bypass operations. Since OEO 2R regeneration compresses the upper and lower noise levels, the two techniques can be combined to balance ASE accumulation with jitter to optimize

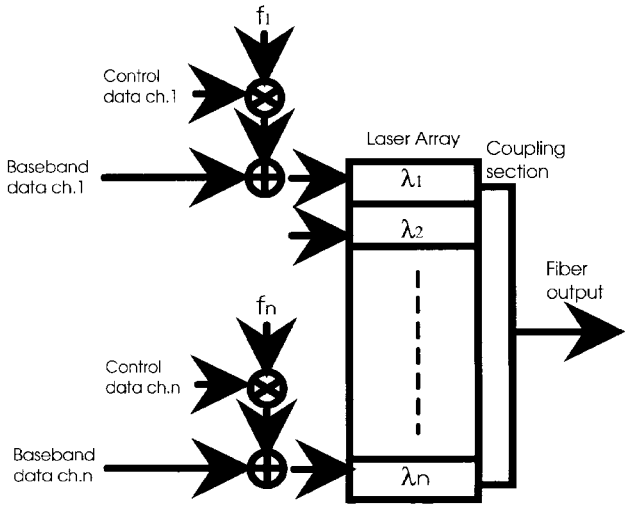

(a)

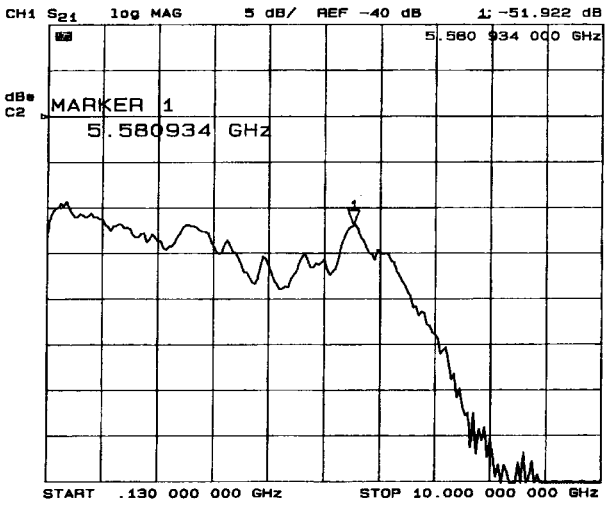

(b)

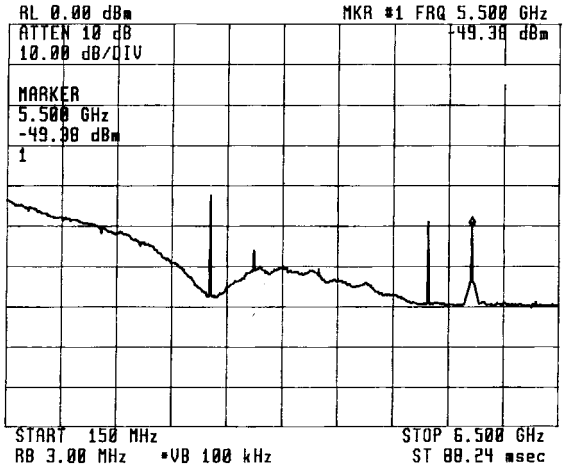

(c)

Fig. 11. (a) Schematic for SCM multiwavelength laser array transmitter; (b) frequency response of the laser array on the subcarrier port; and (c) output spectrum on one channel of the laser array when a 2.5 Gbps baseband signal and a 5.5 Ghz 100 Mb/s subcarrier signal are applied.

lightpath SNR.

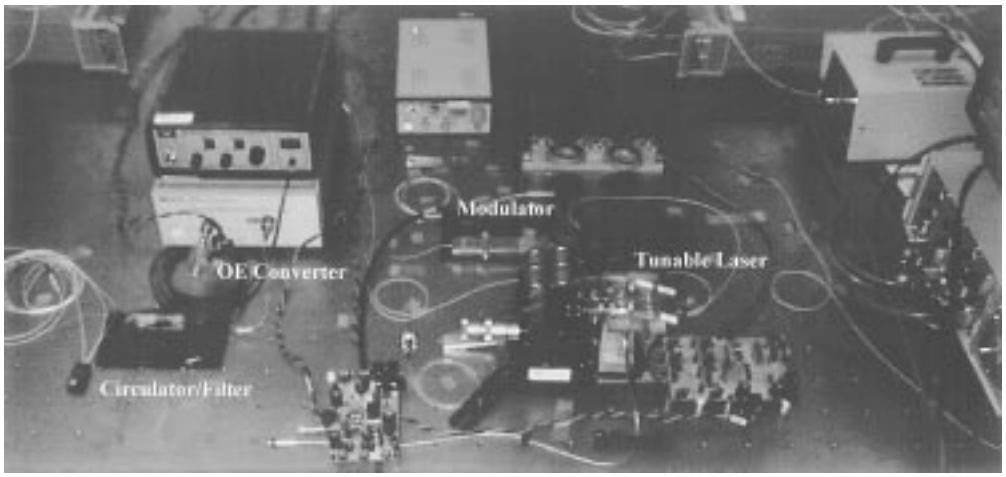

Fig. 12. Photograph of Type III ADM with tunable laser.

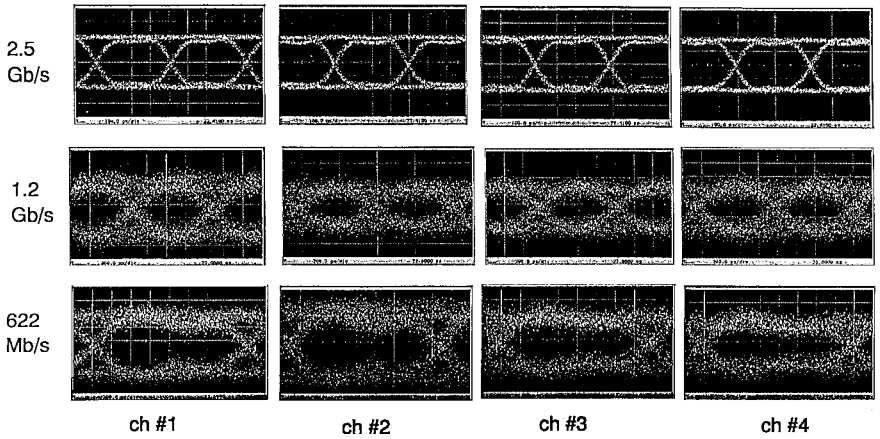

Fig. 13. Eye diagrams illustrating bit rate transparency for 622 Mbps, 1.2 Gbps, and 2.5 Gbps.

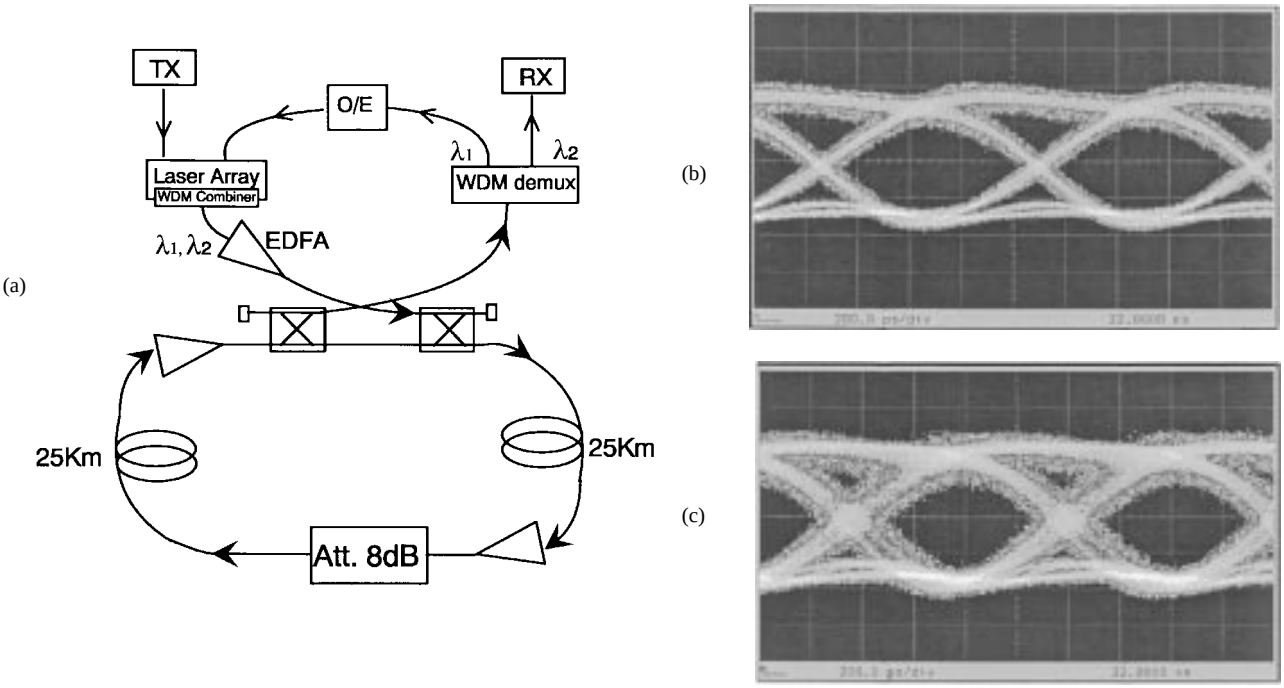

Fig. 14. (a) Experimental setup of two hop bypass with 2R OEO regeneration and wavelength translation, (b) eye diagram after first hop, and (c) eye diagram after second hop.

IV. Network Demonstrations

C. A Three-Node MOSAIC Ring Network Lightpath Demonstration

The three node add/drop multihop lightpath ring network experiment is shown in Fig. 16. The physical topology is shown using solid black lines, and the logical lightpath connection is shown using the light grey lines. The three wavelengths used to support this lightpath are shown in the optical spectrum analyzer insert measured at point (F) in the passive add/drop port. The left most peak is built up ASE from the EDFA gain peaks.

The lightpath originates from the passive add/drop node on λ_1 and is bypass routed through the Type II ADM OEOXC. After propagation through 25 km of single mode dispersion shifted optical fiber, the lightpath is dropped at the Type III ADM and OEO 2R wavelength translated to λ_2. The thresholded PRBS is shown in eye diagram (A). Jitter accumulation following the first OEO 2R conversion is seen in this eye diagram. The lightpath continues on the ring as λ_2, is routed through the passive add/drop port, a 25 km spool of single mode dispersion shifted optical fiber and dropped at the Type II ADM. It is then wavelength demultiplexed, OE converted, and switched by the analog electronic crossbar switch. The eye diagram at this point is indicated and shown in the (B) eye diagram and noise accumulation due to ASE buildup is observed. The analog switch lightpath is then thresholded as shown in eye diagram (B) and illustrates a decrease in the ASE noise buildup and increase in the jitter accumulation due to a second OE 2R regeneration.

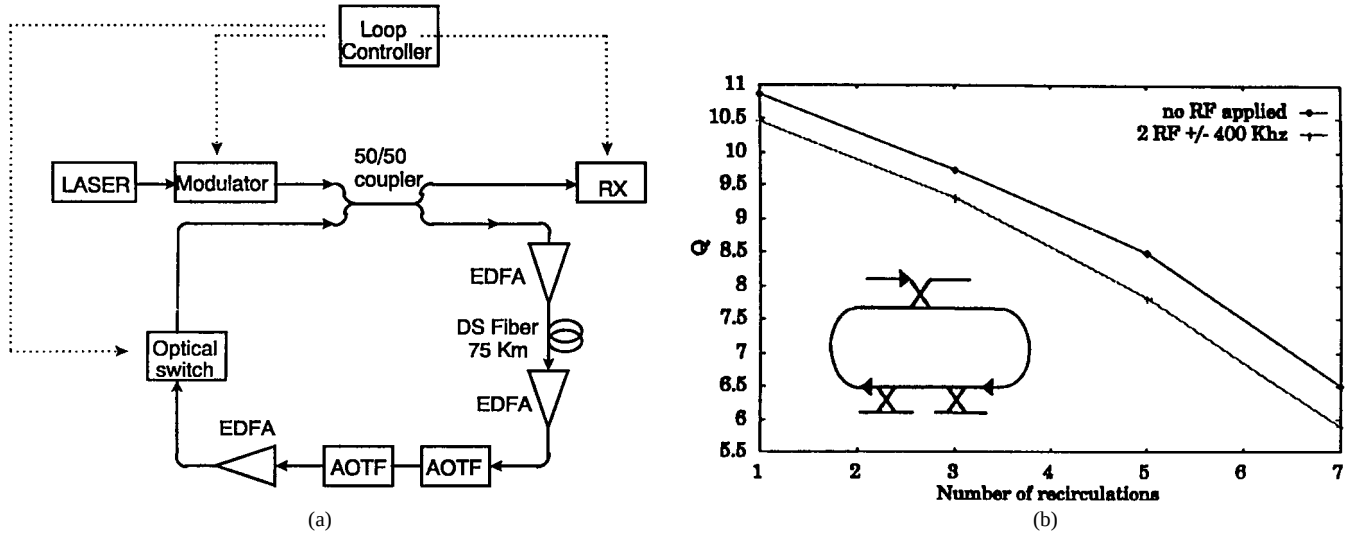

Fig. 15. (a) Experimental setup of seven-hop multichannel optical bypass demonstration and (b) Q as a function of the number of recirculations.

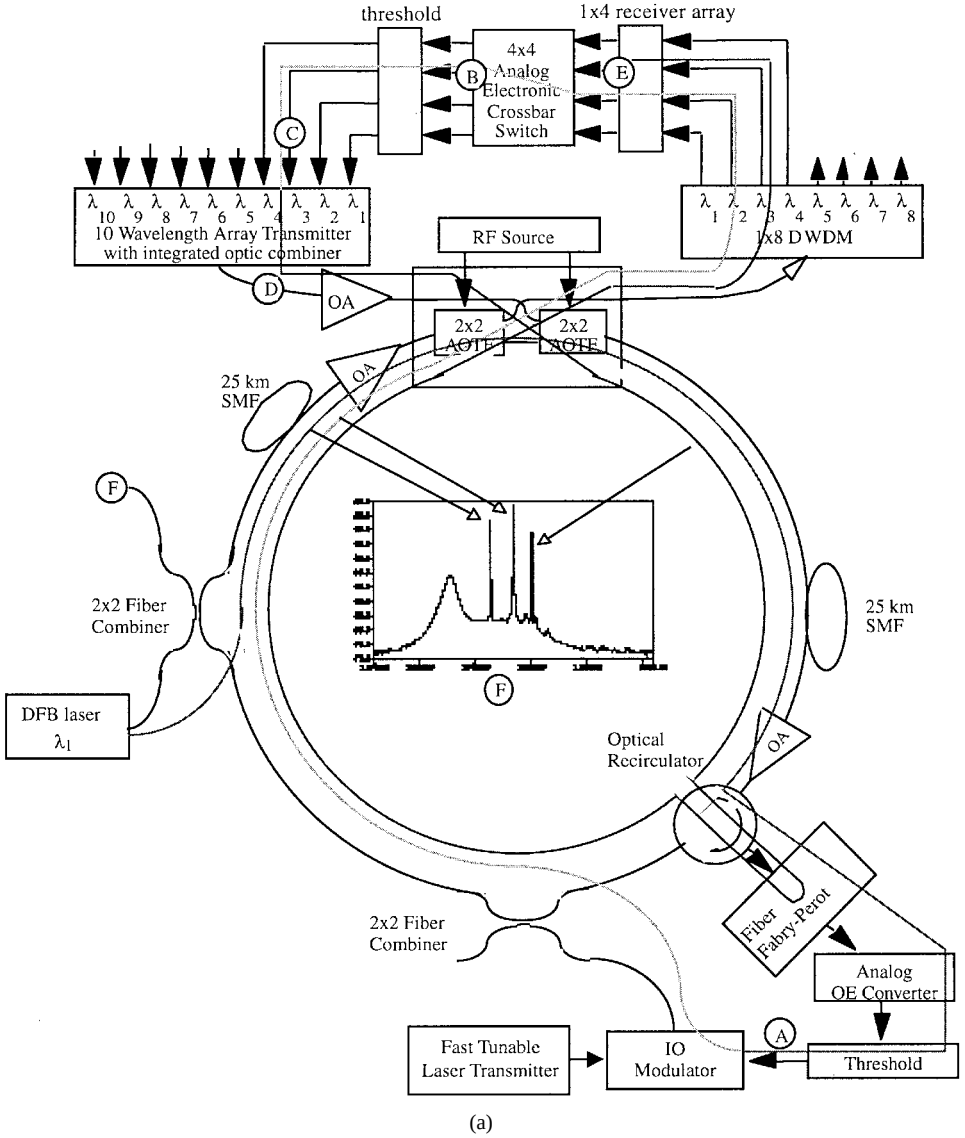

Fig. 16. Schematic of three-node multihop WDM add/drop lightpath experimental demonstration. Dark lines indicate physical connections and light grey lines indicate lightpath. Eye diagrams at various points in network are indicated by A, B, C, D, and E. The optical power spectrum is shown in the center insert F.

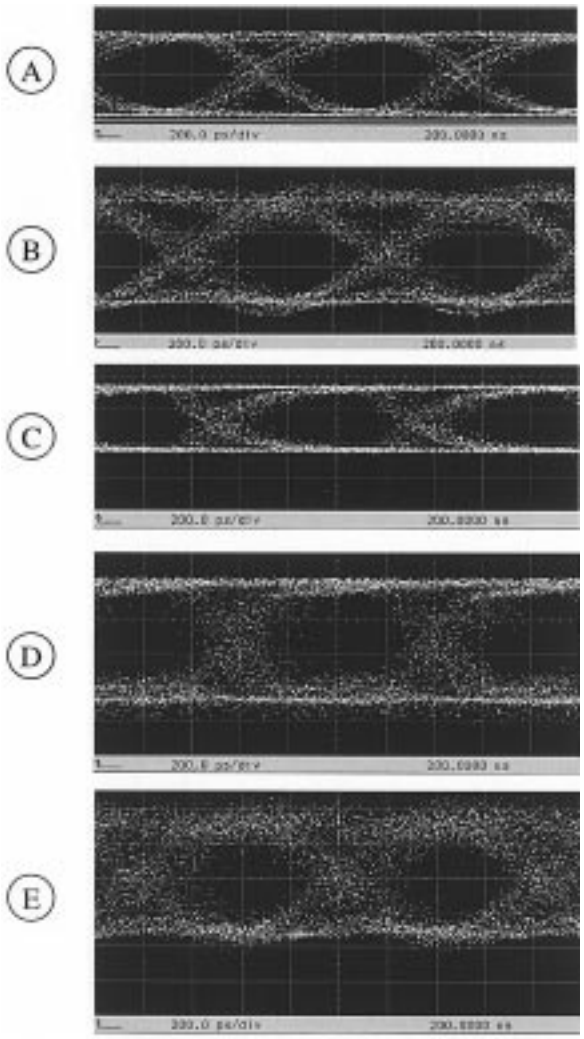

(b)

Fig. 16. (*Continued.*) Schematic of three-node multihop WDM add/drop lightpath experimental demonstration. Dark lines indicate physical connections and light grey lines indicate lightpath. Eye diagrams at various points in network are indicated by A, B, C, D, and E. The optical power spectrum is shown in the center insert F.

The lightpath is translated to λ_3 using the multiwavelength laser transmitter as shown in eye diagram (D). It is added to the network through the dilated AOTF and optically bypassed through the Type III and passive ADM nodes. The lightpath is finally dropped at the Type II node, demultiplexed and OE converted. The resulting eye diagram (E) illustrates that the SNR is still good and that cascaded optical and OEO 2R bypass operations have closed the eye from the top and sides. We measured a BER of 10^{-9} for the transmitted lightpath demonstrating that multiple node, multichannel bit-rate independent lightpaths with wavelength translation can be supported.

V. Summary and Discussions

We have described and experimentally demonstrated the MOSAIC network architecture and its main subsystems and technologies. MOSAIC is a reconfigurable WDM add/drop network with subcarrier multiplexed control that supports multichannel, bit-rate transparent optical lightpaths. Results of a network demonstration show that multihop lightpaths could be established with an end-to-end bit error rate of better than 10^{-9} at 1.2 Gbps. These lightpaths circulated the ring three times with various combinations of optical and OEO bypass and wavelength translation.

Two ADM node architectures were developed and inserted into a three-node network demonstration. The first ADM node architecture is a reconfigurable add/drop multiplexer based on a novel dilated 2×2 acoustooptic filter switch crossconnect and an analog optoelectronic crossconnect that drives a ten-wavelength laser array transmitter up to 2.5 Gbps per wavelength. The second ADM node architecture is a fixed wavelength add/drop multiplexer that utilizes a fast digitally tunable laser transmitter. We demonstrated that both add/drop multiplexers support bit-rate transparent 2R optoelectronic regeneration as well as wavelength translation for multiple hops.

Several key subsystems that support the optical protocol stack, the optical channel section, the multiplexing section, and the optical amplifier section were implemented and demonstrated. Subcarrier multiplexing was used to simultaneously support WDM channel state monitoring, channel equalization, and to carry digital network control information. This subcarrier per wavelength approach supports distributed network control with asynchronous recovery of wavelength, power and control data using a common circuit and requires only a single laser at each users transmitter and a single photodetector at each monitoring or detection point. Important interface technologies were investigated including a digital/RF interface to control the AOTF switches and a photonic/microwave interface to support multichannel subcarrier multiplexing generation and detection.

Systems experiments were performed to demonstrate cascadable 2R optoelectronic regeneration with wavelength translation and cascaded multichannel optical switching with up to 7 hops. The impact of certain physical limitations on bit error rate were measured including multichannel AOTF add/drop penalties and coherent crosstalk due to wavelength reuse.

An important outcome of our experiments was based on mixed optical and electronic switching within a data-rate transparent lightpath. We found that the optical and 2R regeneration techniques affect the lightpath transmission properties in different ways. Optical switching with optical amplification contributes accumulated ASE noise that results in vertical eye closure but does not accumulate timing jitter. OEO 2R regeneration, switching and wavelength translation results in horizontal eye closure due to accumulated jitter but improves the accumulated ASE noise degradation due to thresholding.

Consequently, a balance between optical switching and OEO switching with 2R regeneration and wavelength translation can be chosen to optimize the SNR for a given lightpath. The result is a strong coupling between the optical amplifier protocol layer that ensures high SNR for end-to-end routing and the optical channel protocol layer that establishes lightpaths using wavelength reuse and other available resources. We also found that in general, components and network elements in the optical transport network, performed functions for multiple protocol layers simultaneously.

ACKNOWLEDGMENT

The authors wish to thank K. Pedrotti and K. C. Wang (Rockwell), T. P. Lee (NSF), C. Zah (Corning), C. Dreze and C. Rolland (NorTel) and S. Morasca, S. Bosso, and S. Schmid (Pirelli Cavi S.p.A) for their valuable support and experience. They also thank J. Copeland (Georgia Tech) for his support in this effort and C. Juckett, B. House, and S. Halpern for their electronic circuit support.

REFERENCES

[1] A. A. M. Saleh, "Transparent optical networks for the next generation information infrastructure," in *Proc. OFC'95*, San Diego, CA, 1995, p. ThE1.

[2] R. Ramaswami and K. N. Sivarajan, *Optical Networks.* San Mateo, CA: Morgan Kaufmann, 1997.

[3] S. Johansson, M. Lindblom, P. Granestrand, B. Lagerstrom, and L. Thylen, "Optical cross-connect system in broad-band networks: System concept and demonstrators description," *J. Lightwave Technol.,* vol. 11, pp. 688–713, May 1993.

[4] G. K. Chang, G. Ellinas, J. K. Gamelin, M. Z. Iqbal, and C. A. Brackett, "Multiwavelength reconfigurable WDM/ATM/SONET network testbed," *J. Lightwave Technol.*, vol. 14, pp. 1320–1340, June 1996.

[5] S. Johansson, "Transport network involving reconfigurable WDM network layer—A European demonstration," *J. Lightwave Technol.*, vol. 14, pp. 1341–1348, June 1996.

[6] R. E. Wagner, "Overview of multiwavelength optical networking (MONET) program," in *Proc. LEOS '96*, Boston, MA, Nov. 1996, pp. 56–57.

[7] J. Gamelin, M. Goodman, J. Jackel, B. Pathak, G. K. Chang, W. J. Tomlinson, R. Cordell, C. E. Zah, T. P. Lee, C. Brackett, C. Dreze, D. Pollex, J. Stich, H. Willemson, K. Pedrotti, K. C. Wang, R. Walden, W. Stanchina, D. Fritz, R. Ade, R. Hobbs, R. Haigh, K. McCammon, and W. Lennon, "8-channel reconfigurable WDM networking demonstration with wavelength translation and electronic multicasing at 2.5 Gbps," in *Proc. Conf. Optical Fibers and Communications*, San Jose, CA, 1996, pp. PD29–2.

[8] "Draft Rec. G. LON: Functional characteristic of interoffice and long-haul systems using optical amplifiers, including optical multiplexing," Tech. Rep. ITU-T SG25/WP4, 1996.

[9] A. A. M. Saleh, "Overview of the MONET multiwavelength optical networking program," in *Proc. OFC '96*, San Jose, CA, 1996, p. ThI3.

[10] G. R. Hill, P. J. Chidgey, F. Kaufhold, T. Lynch, O. Sahlen, M. J. Ingers, L. Gernandez, S. Rotolo, A. Antonielli, S. Tebaldini, E. Vessoni, R. Caddedu, N. Caponio, F. Testa, A. Acavennec, M. J. O'Mahony, A. Y. J. Zhou, W. Sohler, U. Rust, and H. Herrman, "A transport network layer based on optical network elements," *J. Lightwave Technol.*, vol. 11, pp. 667–679, 1993.

[11] N. R. Dono, J. P. E. Green, K. Liu, R. Ramaswami, and F. F.-K. Tong, "A wavelength division multiple access network for computer communication," *IEEE J. Select. Areas Commun.*, vol. 8, pp. 983–993, Aug. 1990.

[12] M. Cerisola, T. K. Fong, R. T. Hofmeister, L. G. Kazovsky, C. L. Lu, P. Poggiolini, and D. J. M. Sabido, "CORD—A WDM optical network: Control mechanism using subcarrier multiplexing and novel synchronization solutions," in *Proc. Int. Conf. Communications*, Seattle, WA, June 1995, pp. 261–265.

[13] D. J. Blumenthal, J. Laskar, R. Gaudino, S. Han, M. D. Shell, and M. D. Vaughn, "Fiber-optic links supporting baseband data and subcarrier-multiplexed control channels and the impact of MMIC photonic/microwave interfaces," *IEEE Trans. Microwave Theory Tech.*, vol. 45, pp. 1443–1452, Aug. 1997.

[14] A. R. Chraplyvy, "Limitation on lightwave communications imposed by optical-fiber nonlinearities," *J. Lightwave Technol.*, vol. 8, pp. 1548–1557, Oct. 1990.

[15] G. H. Smith and D. Novak, "Broad-band millimeter-wave (38 GHz) fiber-wireless transmission system using electrical and optical SSB modulation to overcome dispersion effects," *IEEE Photon. Technol. Lett.*, vol. 10, pp. 141–143, Jan. 1998.

[16] L. Y. Lin, M. C. Wu, T. Itoh, T. A. Vang, R. E. Muller, D. L. Sivco, and A. Y. Cho, "High-power high-speed photodetectors-design, analysis, and experimental demonstration," *IEEE Trans. Microwave Theory Tech.*, vol. 45, pp. 1320–1331, Aug. 1997.

[17] S. Morasca, D. Scarano, and S. Schmid, "Application of $LiNbO_3$ acousto-optic tunable switches and filters in WDM transmission networks at high bit rates," presented at 8th Tyrrenian Int. Workshop on Digital Communication, Lerici (SP), Italy, 1996.

[18] R. Gaudino and D. J. Blumenthal, "A novel AOTF-based multichannel add–drop node and its cascadability in WDM ring networks," in *Proc. 23rd Eur. Conf. Optical Communications (ECOC '97)*, Edinburgh, 1997, vol. 4, pp. 77–80.

[19] P. J. Rigole, M. Shell, S. Nilsson, D. J. Blumenthal, and E. Berglind, "Fast wavelength witching in a widely tunable GCSR laser using a pulse pre-distortion technique," in *Proc. Optical Fiber Communications Conf. (OFC'97)*, 1997, pp. 231–232.

[20] C. L. Lu, D. J. M. Sabido, P. Poggiolini, R. T. Hofmeister, and L. G. Kazovsky, "CORD—A WDMA optical network: Subcarrier-based signaling and control scheme," *IEEE J. Photon. Technol. Lett.*, vol. 7, pp. 555–557, May 1995.

[21] D. A. Smith *et al.*, "Evolution of the acousto-optic wavelength routing switch," *J. Lightwave Technol.*, vol. 14, pp. 1005–1018, June 1996.

[22] F. Tian and H. Herrmann, "International interference in multiwavelength operation of integrated acousto-optic filter and switches," *J. Lightwave Technol.*, vol. 13, pp. 1146–1153, June 1995.

[23] J. L. Jackel, J. E. Baran, G. K. Chang, M. Z. Iqbal, G. H. Song, W. J. Tomlinson, and R. Ade, "Multichannel operation of AOTF switches: Reducing channel-to-channel interaction," *IEEE Photon. Technol. Lett.*, vol. 4, pp. 370–373, Apr. 1995.

[24] J. Sharony, K. Cheung, and T. Stern, "The wavelength dilation concept in lightwave networks: Implementations and system considerations," *J. Lightwave Technol.*, vol. 11, pp. 900–907, June 1993.

[25] E. L. Goldstein and L. Eskildsen, "Scaling limitations in transparent optical networks due to low-level crosstalk," *IEEE Photon. Technol. Lett.*, vol. 7, pp. 93–94, Jan. 1995.

[26] D. J. Blumenthal, M. Shell, Q. Gao, M. Vaughn, A. Wang, P. Rigole, and S. Nilsson, "Experimental demonstration of an all-optical multihop routing node for wavelength routed networks," presented at Conf. Optical Fibers and Communications, San Jose, CA, 1996.

[27] A. E. Willner and S. M. Hwang, "Optically-amplified WDM ring network incorporating channel-dropping filters," *IEEE Photon. Technol. Lett.*, vol. 6, June 1994.

[28] S. F. Su, R. Olshansky, G. Joyce, D. A. Smith, and J. E. Baran, "Gain equalization in multiwavelength lightwave systems using acoustooptic tunable filters," *IEEE Photon Technol. Lett.*, vol. 4, pp. 217–296, Mar. 1992.

[29] T. Hayashi *et al.*, "Reducing electrical crosstalk in laser-diode array modules by using a film-carrier interconnection," *J. Lightwave Technol.*, vol. 13, pp. 1885–1891, Sept. 1995.

[30] K. C. Wang, K. D. Pedrotti, and K. Runge, "High speed A1GaAs/GaAs HBT circuits for optical fiber communications," vol. 1, pp. 39–40, Nov. 1994.

[31] M. Shell and D. J. Blumenthal, "Improved multichannel performance in a 10-wavelength 25 Gbps multichannel laser array transmitter module," presented at LEOS Summer Topical Meeting on WDM Component Technology, Aug. 1997.

[32] P. J. Rigole, S. Nillsson, L. Backbom, T. Klinga, J. Wallin, B. Stalnacke, E. Berglind, and B. Stoltz, "114 nm wavelength tuning rande of a vertical grating assisted codirectional coupler laser with a super structure grating distributed Bragg reflector," *IEEE Photon. Technol. Lett.*, vol. 7, pp. 697–699, July 1995.

[33] P. E. J. Green, F. H. Janniello, and R. Ramaswami, "WDM protocol-transparent distance extension using R2 remodulation," *IEEE J. Select. Areas Commun.*, vol. 14, pp. 962–967, June 1996.

[34] L. Thlyen, P. Ohlen, and E. Berglind, "Role of simple nondigital optoelectronic repeaters in scalable, transparent optical networks," in *Conf. Proc. Laser Electr. Optic Soc. Ann. Meet.*, 1996, vol. 1.

Roberto Gaudino received the Laurea and the Ph.D. degrees in electrical engineering from the Politecnico di Torino, Turin, Italy, in 1993 and 1998, respectively. In 1997 he spent a year as a visiting scholar at the Georgia Institute of Technology, where he worked on topics related to optical networks in the optical communication and photonic network (OCPN) group.

He is currently with the Optical Communications Group at the Politecnico di Torino, where he conducts research in the area of optical communications.

May Len received the B.Sc. degree in electrical engineering from the Georgia Institute of Technology, Atlanta, in 1998.

She is currently with Motorola.

Geoffrey Desa was born in 1978 in Bombay, India. He is currently pursuing the B.Sc. degree in electrical engineering at the Georgia Institute of Technology, Atlanta, with a focus on optical communications and RF networks.

He is a member of the optical communications and photonic networks research (OCPN) group and has been involved in the optical interconnect and photoreceiver sections of MOSAIC. His research interests include optical recirculating loops, the manufacture of LCD display prototypes, and the modeling of subthreshold inversion characteristics of MOSFET's.

Michael Shell (S'95–M'97) photograph and biography not available at the time of publication.

Daniel J. Blumenthal (S'91–M'93–SM'97) received the B.S.E.E. degree from the University of Rochester, NY, in 1981, the M.S.E.E. degree from Columbia University, New York, NY, in 1988, and the Ph.D. degree from the University of Colorado at Boulder in 1993.

In 1981, he joined StorageTek of Louisville, CO, where he was engaged in research and development in optical data storage systems. In 1986, he worked at Columbia University as a Research Engineer in the areas of photonic switching systems and ultra-fast all-optical networks and signal processing. In 1990, he was a Graduate Research Assistant working on multiwavelength photonic switched interconnects for distributed computing applications. From 1993 to 1997, he was Assistant Professor in the School of Electrical and Computer Engineering at the Georgia Institute of Technology. Currently, he is Associate Professor in the Department of Electrical and Computer Engineering at the University of California at Santa Barbara and heads the Optical Communications and Photonic Networks (OCPN) Research Group. His current research areas are in optical communications, wavelength conversion in semiconductor devices, optical subcarrier multiplexing, and optical information processing. He has authored or co-authored more than 40 papers in these and related areas.

Dr. Blumenthal is recipient of an NSF Young Investigator (NYI) Award and a Office of Naval Research Young Investigator Program (YIP) Award. He is currently an Associate Editor for IEEE PHOTONICS TECHNOLOGY LETTERS and Associate Editor for IEEE TRANSACTIONS ON COMMUNICATIONS, and is Guest Editor for the JOURNAL OF LIGHTWAVE TECHNOLOGY Special Issue in Photonic Packet Switching. He has served on numerous conference committees including the program committee for the 1997, 1998, and 1999 Conference on Optical Fiber Communications (OFC). He is a member of the Optical Society of America and the IEEE Lasers and Electrooptic Society.